

Present and Future Long Baseline Neutrino Experiment in Japan

Takashi Kobayashi

for K2K collaboration and JHF ν working group

Institute for Particle and Nuclear Studies, KEK, 1-1 Oho, Tsukuba, 305-0801, Japan

Abstract

The K2K experiment is the first accelerator-based long baseline neutrino experiment aiming to confirm the evidence of neutrino oscillation found in the atmospheric neutrino observation. The ν_μ beam of ~ 1 GeV is produced at KEK and observed by Super-Kamiokande (SK) at 250 km distance. From June 1999 to June 2000, we have accumulated about 23% of proposed number of protons on target. We observed 28 neutrino events in SK which originate at KEK. Expected number of events are $37.8^{+3.5}_{-3.8}$. As a next generation experiment, we plan a neutrino oscillation experiment with baseline length of 295 km using 50 GeV PS in Japan Hadron Facility, which is approved last year, and SK. Using the ~ 1 MW PS, we expect about 2 orders of magnitude higher neutrino flux than K2K. This high intensity beam enables us to determine oscillation parameters in ν_μ disappearance and explore ν_e appearance with unprecedented precision and reach. Current design of the neutrino facility and its physics potential are introduced.

1 Introduction

The significant deficit of upward going atmospheric muon neutrino observed at Super-Kamiokande (SK) is the first evidence of the phenomena beyond the standard electroweak theory: neutrino oscillation ¹⁾. Existence of neutrino oscillation means nothing but non zero neutrino mass and lepton flavor violation ²⁾. The standard model is required to be extended anyhow. Therefore it is an urgent and important task to firmly confirm the SK results with different systematics. For that purpose some long baseline experiments have been planned in which ν_μ beam is produced by an accelerator, flown several 100 km and checked its flavor contents at the far site. As the first of those, the K2K, KEK to Kamioka, long baseline neutrino oscillation experiment has been running since 1999 ³⁾. In the experiment ν_μ beam is produced by 12 GeV proton synchrotron (PS) in High Energy Accelerator Research Organization (KEK), Japan and detected by SK at 250 km distance. The mean beam energy is 1.3 GeV and the maximum sensitivity to mass square difference Δm^2 is at $\sim 7 \times 10^{-3} \text{ eV}^2$. The sensitive region of K2K covers most of the allowed region by SK. We report here latest results from K2K.

After once those “first generation” experiments confirmed the SK results definitely, possible next steps for long baseline experiments are

1. establish (or deny) scenario of 3 generation mixing,
2. precision measurements of oscillation parameters,
3. search for CP violation in lepton sector.

The first item is achieved by high precision measurement of oscillation pattern in ν_μ disappearance spectrum, discovery of ν_e appearance, and measurement of neutral current (NC) interactions. Any deviations from expectations of standard 3 flavor scenario indicate existence of new physics. Aiming at the above items, a “second generation” long baseline neutrino oscillation experiment is planned in Japan ⁴⁾. The ν_μ beam is produced by $\sim 1 \text{ MW}$ 50 GeV PS in Japan Hadron Facility (JHF) which is approved in December 2000 ⁵⁾. The intensity of the neutrino beam is expected to be about 2 orders of magnitudes higher than K2K. The facility will be completed by 2006. At the first phase of the project, the far detector is SK at 295 km distance. In the second phase, we plan to use upgraded 4 MW PS and 1 Mt “Hyper-Kamiokande” ⁶⁾. Currently the design work of the neutrino facility and the study of the physics potential are going on. Here we present the current design of the facility and the results of the studies.

2 Neutrino Oscillation

When a weak eigenstate $|\nu_l\rangle$ is expressed as mixing of mass eigenstates $|\nu_i\rangle$, $|\nu_l\rangle = \sum_i U_{li} \cdot |\nu_i\rangle$ ($l = e, \mu, \tau, i = 1, 2, 3$) probability for a flavor eigenstate $|\nu_l\rangle$ at $t = 0$ changes its flavor to m at time t (or at distance L) is

$$P(\nu_l \rightarrow \nu_m) = |\langle \nu_m(t) | \nu_l(0) \rangle|^2, \quad (1)$$

$$= \delta_{ml} - 2 \sum_{i < j} \text{Re} \left[(U_{mi}^* U_{li}) (U_{mj} U_{lj}^*) \left\{ 1 - \exp \left(-i \frac{\Delta m_{ij}^2}{2E_\nu} L \right) \right\} \right], \quad (2)$$

where E_ν is neutrino energy and $\Delta m_{ij}^2 \equiv m_i^2 - m_j^2$, and m_i is mass eigenvalue of the state $|\nu_i\rangle$. The unitary matrix U can be parametrized by three mixing angles θ_{12} , θ_{23} and θ_{13} and one CPV phase δ ⁷⁾;

$$U = \begin{pmatrix} 1 & 0 & 0 \\ 0 & C_{23} & S_{23} \\ 0 & -S_{23} & C_{23} \end{pmatrix} \begin{pmatrix} C_{13} & 0 & S_{13} e^{-i\delta} \\ 0 & 1 & 0 \\ -S_{13} e^{i\delta} & 0 & C_{13} \end{pmatrix}, \begin{pmatrix} C_{12} & S_{12} & 0 \\ -S_{12} & C_{12} & 0 \\ 0 & 0 & 1 \end{pmatrix}, \quad (3)$$

where S_{ij} (C_{ij}) stands for $\sin\theta_{ij}$ ($\cos\theta_{ij}$). The solar ⁸⁾ and atmospheric ¹⁾ neutrino data indicate that

$$\Delta m_{\text{sol}}^2 = \Delta m_{12}^2 \ll \Delta m_{23}^2 \simeq \Delta m_{13}^2 = \Delta m_{\text{atm}}^2. \quad (4)$$

In this case, when the energy scale of an experiment is at $E_\nu \simeq \Delta m_{23}^2 \cdot L$, contribution from Δm_{12}^2 terms becomes negligible and oscillation probabilities relevant to the experiment can be expressed by rather simple formula;

$$P(\nu_\mu \rightarrow \nu_\mu) = 1 - P(\nu_\mu \rightarrow \nu_e) - P(\nu_\mu \rightarrow \nu_\tau) - P(\nu_\mu \rightarrow \nu_s) \quad (5)$$

$$P(\nu_\mu \rightarrow \nu_\tau) \simeq \cos^4\theta_{13} \cdot \sin^2 2\theta_{23} \cdot \sin^2 \Phi_{23} \equiv \sin^2 2\theta_{\mu\tau} \cdot \sin^2 \Phi_{23}, \quad (6)$$

$$P(\nu_\mu \rightarrow \nu_e) \simeq \sin^2\theta_{23} \cdot \sin^2 2\theta_{13} \cdot \sin^2 \Phi_{23} \equiv \sin^2 2\theta_{\mu e} \cdot \sin^2 \Phi_{23}, \quad (7)$$

$$P(\nu_e \rightarrow \nu_e) \simeq 1 - \sin^2 2\theta_{13} \cdot \sin^2 \Phi_{23}, \quad (8)$$

where $\Phi_{ij} \equiv \Delta m_{ij}^2 L / 4E_\nu = 1.27 \Delta m_{ij}^2 [\text{eV}^2] L [\text{km}] / E_\nu [\text{GeV}]$. If the effective mixing angles $\theta_{\mu\tau}$ and $\theta_{\mu e}$ are defined as in eq. (5) and (7), the expressions reduces to the case of 2 flavor oscillation.

Experimental constraints obtained from ν_μ disappearance in the atmospheric neutrino are $\sin^2 2\theta_{\mu\tau} > 0.89$ and $1.6 \times 10^{-3} < \Delta m_{23}^2 < 4 \times 10^{-3} \text{ eV}^2$ ¹⁾. There are several allowed regions in oscillation parameter space by observations of solar neutrino. But even for the largest Δm_{sol}^2 solution, $\Delta m_{\text{sol}}^2 \lesssim 1.6 \times 10^{-4} \text{ eV}^2$ ⁸⁾. Constraint on θ_{13} comes from reactor $\bar{\nu}_e$ disappearance experiments. As can be seen

in eq. (8), $\bar{\nu}_e$ disappearance directly measures θ_{13} . Current limit is $\sin^2 2\theta_{13} < 0.05$ for $\Delta m_{23}^2 \simeq 6 \times 10^{-3} \text{ eV}^2$ and $\sin^2 2\theta_{13} \lesssim 0.12$ at $\Delta m_{23}^2 \simeq 3 \times 10^{-3} \text{ eV}^2$ at 90 % C.L. Since θ_{13} is very small and atmospheric neutrino data indicates almost full mixing $\theta_{23} \simeq \pi/4$, the two flavor mixing angles are directly related to 3 flavor angles as $\sin^2 2\theta_{\mu\tau} \simeq \sin^2 2\theta_{23}$, and $\sin^2 2\theta_{\mu e} \simeq \frac{1}{2} \sin^2 2\theta_{13}$.

3 Present Long Baseline Neutrino Experiment — K2K —

3.1 Experimental setup

Neutrino facility in the KEK site is drawn in Fig. 1. Muon neutrino beam

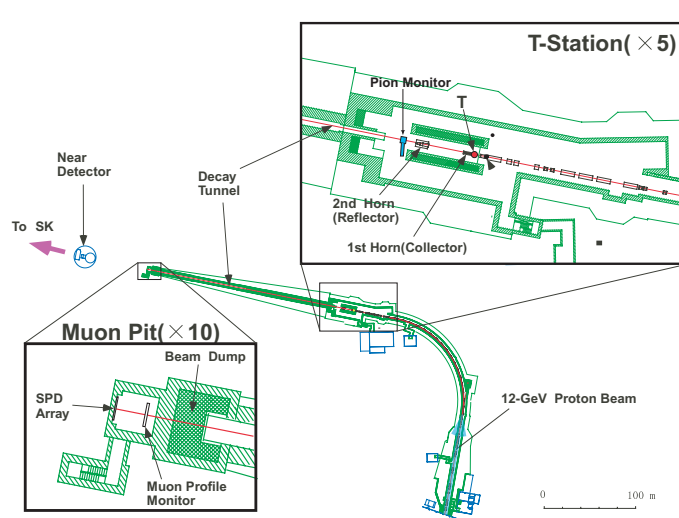


Figure 1: Neutrino facility in KEK.

is produced at KEK by using the 12 GeV (kinetic energy) PS. The proton beam is extracted from the PS in single turn with 2.2 sec cycle. A spill is 1.1 μsec width and consists of nine bunches. The design intensity of the proton beam at the production target is 6×10^{12} protons/pulse (ppp). The target is 66 cm long Al rod. The diameter of the target is 2 cm for runs in June 1999, and 3 cm since November 1999. Positive secondary pions are focused by two electromagnetic horns⁹⁾. Both horns are operated by pulsed current of ~ 1 msec width and 200 kA peak for June 1999 run and 250 kA peak for runs since Nov. 1999. The target is embedded in the first horn and plays a role as an inner conductor. The length of the decay tunnel is 200 m. A beam dump of 3-m thick iron followed by 2 m thick concrete is placed at the end of the decay pipe. Most particles except muons above 5 GeV stop in the dump. Beam line components are aligned with Global Positioning System (GPS)¹⁰⁾. The precision of the GPS survey is $\lesssim 0.01$ mrad while that of the civil construction is

$\lesssim 0.1$ mrad. Expected neutrino spectra and the radial dependence of flux at SK are plotted in Fig. 2. The average neutrino energy is 1.3 GeV. As can be seen in the figure, the neutrino flux is almost constant within 3 mrad (~ 750 m) at SK. The purity of ν_μ in the beam is estimated by Monte Carlo (MC) simulation to be 98.2% and ν_e contamination to be 1.3%.

At just behind the beam dump, two types of muon monitors (MUMONs) are installed. One is a 2 m \times 2 m segmented ionization chamber. Horizontal and vertical strips are 5 cm width. The other is array of silicon pad detectors as shown in Fig. 3. The MUMONs provide spill-by-spill monitoring of the beam profile and intensity. Pion monitor (PIMON) is a gas Čerenkov detector occasionally placed just downstream of the 2nd horn in the target station as shown in the inset of Fig. 1¹¹⁾. Its purpose is to measure momentum and angular distribution of secondary pions, $N(p_\pi, \theta_\pi)$. Once the distribution is known, one can predict neutrino spectra at any distance in principle without relying on any hadron production model. Schematic view of PIMON is shown in Fig. 3. The Čerenkov light from secondary particles is

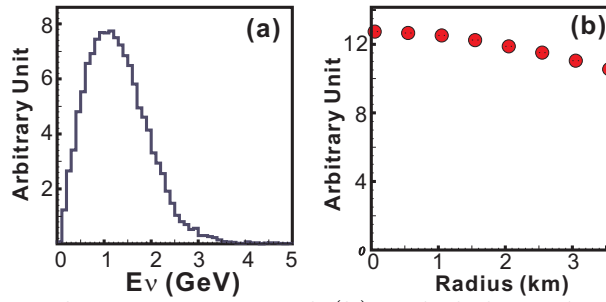


Figure 2: (a) Expected ν_μ spectrum and (b) radial dependence of the flux at far site.

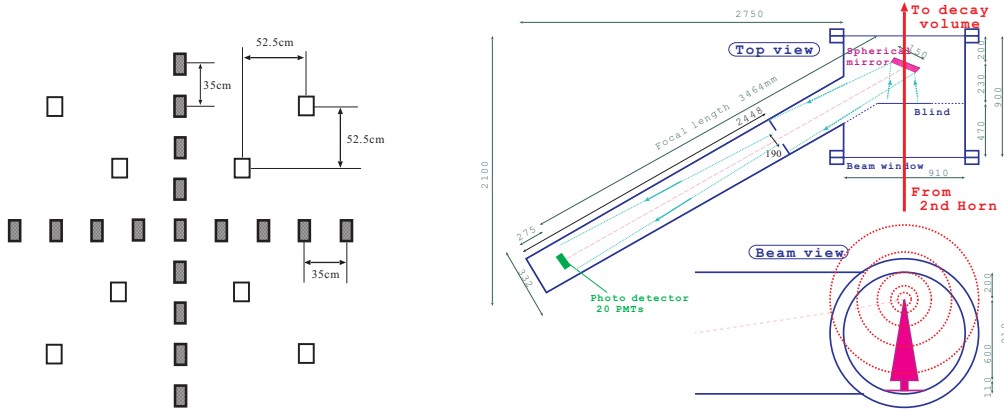


Figure 3: (Left) Front view of silicon pad detectors for muon monitoring. Hatched pads are 10 \times 10 mm² and open boxes are 34 \times 30.5 mm². (Right) Schematic view of pion monitor.

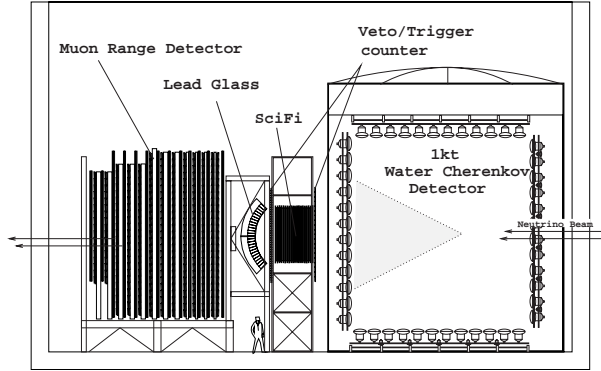


Figure 4: Front neutrino detector.

reflected by spherical mirror in the gas volume. The reflected light is detected by 1-dim PMT array placed at the focal plane of the mirror. In order to cover various p_π region, measurements are performed at various refractive indices by adjusting the gas pressure. However the refractive index can not be raised above 1.00264 because 12 GeV primary protons start emitting Čerenkov light and overwhelm the pions. Therefore PIMON is insensitive in the range $p_\pi \lesssim 2$ GeV/c ($E_\nu \lesssim 1$ GeV). To eliminate the possible errors in the absolute measurement of number of pions, we use the flux ratio at SK to FD, $R_\Phi(E_\nu) \equiv \Phi_{\text{SK}}(E_\nu)/\Phi_{\text{FD}}(E_\nu)$ as a result of the PIMON.

The front neutrino detector (FD) is located at 300 m downstream from the target. The FD consists of a 1 kt water Čerenkov detector (1kt) and a fine grained detector (FGD) as shown in Fig. 4. The purposes of the FD are to measure absolute ν_μ flux as a function of energy, i.e. $\Phi_{\text{FD}}(E_\nu)$, ν_e contamination, and to monitor beam direction by measuring vertex distribution. The 1kt is a ring imaging Čerenkov detector which works with the same principle as SK. The detector volume of $8.6 \text{ m}^\phi \times 8.5 \text{ m}$ is filled with pure water and is viewed by 680 20-inch PMT's. The fiducial mass is 25 t. The FGD is composed of a scintillation fiber tracker (SciFi), VETO/TRIG scintillater walls, a lead glass (LG) detector and a muon range detector (MRD). The SciFi is a stack of 6-cm thick water in Al water container and sheets of staggered fibers ¹²⁾. The total mass of the water is 6 t. The position resolution of SciFi is measured to be 0.55 mm using cosmic-ray data taken after installation. The purpose of the LG detector is to identify electrons from ν_e interactions and to measure their energies. The energy resolution is $\sim 10\%/\sqrt{E}$ [GeV]. The MRD is a stack of 10- or 20-cm thick $8 \times 8 \text{ m}^2$ iron plates and drift chambers. The total mass of the iron plates is 915 t. The large mass of MRD gives high event rate and enables us to monitor the event rate stability. Also because the area of the MRD is very

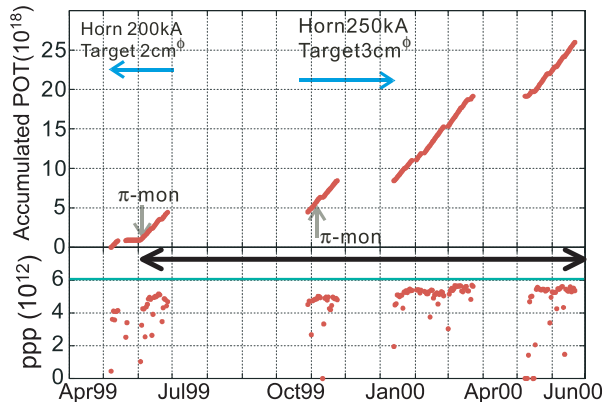


Figure 5: Delivered beam history.

wide, we can monitor the neutrino beam profile.

The far detector, SK, is a ring imaging water Čerenkov detector located 1000 m underground (2700 m water equivalent) at 250 km away from KEK. It consists of inner detector (ID) and outer detector (OD). The ID is a cylindrical water tank of 36 m in diameter and 34 m in height which is viewed by 11146 20-inch PMT's. The fiducial mass is 22.5 kt. The OD is a water Čerenkov detector which surrounds the ID and is equipped with 8 inch PMTs. It detects entering activities and provides information to veto them in offline process. Detailed description of the detector can be found elsewhere ¹⁾.

3.2 Results

History of delivered beam is plotted in Fig. 5. The first fast extraction succeeded on Feb. 3rd, 1999. After engineering runs, we started physics run in June, 1999. Until June 2000, 22.9×10^{18} protons on target (POT) has been accumulated with SK live. The instantaneous intensity gradually increased and almost reached at the design intensity of 6×10^{12} ppp. In June 1999, the horn current was 200 kA and the target diameter was 2 cm $^\phi$. Since October 1999, horn current has been the design current of 250 kA and the target is 3 cm $^\phi$. PIMON measurements were done in the beginning of June and November 1999 runs.

At SK, we looked for neutrino events with all secondary particles contained in the ID (fully contained: FC). The selection criteria are: a) no detector activity within 30 μ sec before the event, b) total collected photo-electron (p.e.) in 300 ns time window > 200 , c) number of hit PMTs in the largest hit cluster in OD < 10 , d) observed electron equivalent energy > 30 MeV, e) fiducial cut (distance of the reconstructed vertex from the wall > 200 cm). In order to identify the events induced

by neutrinos from KEK, time of every beam spill start (T_{spl}) and every SK event trigger (T_{SK}) are recorded by using GPS¹³). We expect $\Delta T \equiv T_{SK} - T_{spl} - TOF$ to be between 0 and 1.1 μsec , where $TOF \simeq 830 \mu\text{sec}$ is time of flight of neutrino from KEK to Kamioka. Fig. 6 shows the ΔT distributions of samples after the cuts a), b) and e). Since the measured uncertainty of the GPS time is $< 200 \text{ ns}$, time

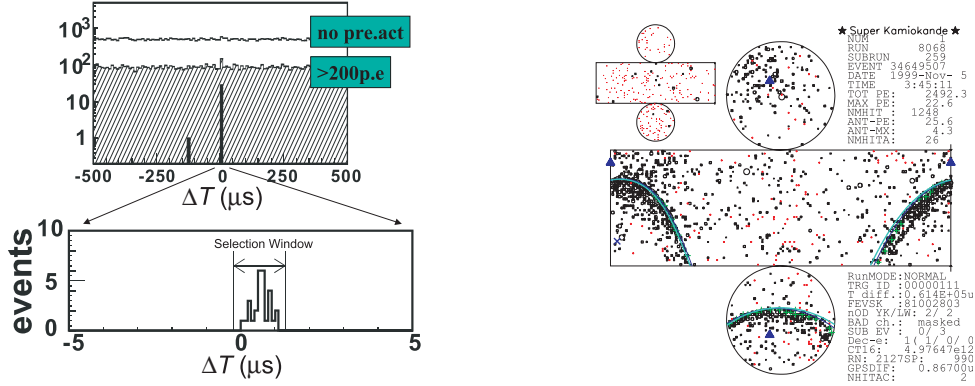


Figure 6: (Left) ΔT distribution. (Right) A candidate of fully contained single ring μ -like event in fiducial volume.

window for the event selection is set to $-0.2 < \Delta T < 1.3 \mu\text{sec}$. We found 28 events which satisfy all the criteria in the signal timing window. Event display of one of the candidates is shown in Fig. 6. It is single ring μ -like event with the reconstructed muon momentum of 467 MeV/c.

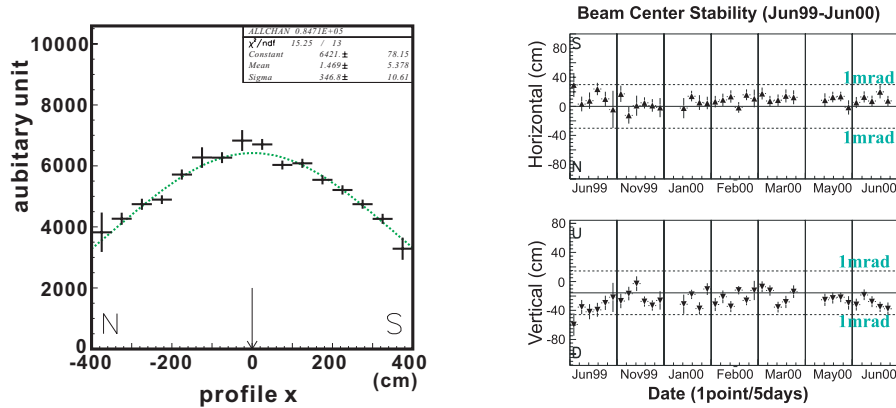


Figure 7: (Left) Beam profile. Points are measured by MRD Iron events and curve is fitted Gaussian function. (Right) stability of profile center during long period.

Stability of the beam is mainly monitored by using neutrino events in MRD Iron plates owing to its high statistics. Vertex distribution of MRD Iron events, that is equivalent to neutrino beam profile, is shown in Fig. 7. Beam center is obtained

by fitting Gaussian function to the profile. The beam center agrees well with the SK direction within systematic uncertainty of 20 cm (which corresponds to ~ 0.7 mrad). The stability of the beam center is demonstrated also in Fig. 7. The beam center has been stable within ± 1 mrad throughout the running period. Plots in Fig. 8

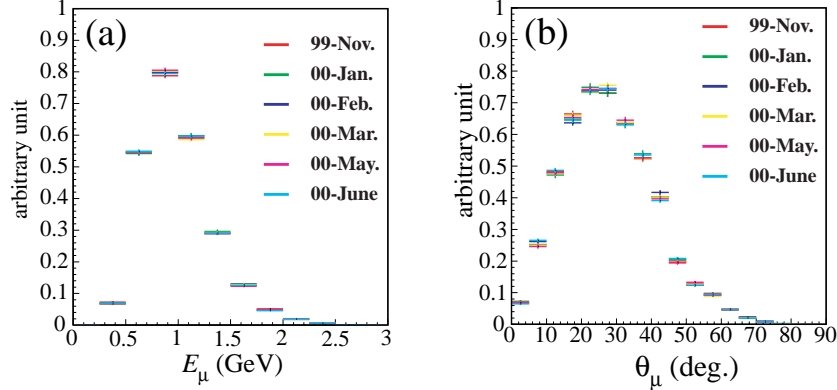


Figure 8: Muon (a) energy spectra and (b) angular distributions of ν_μ interactions in MRD Iron plates for each month.

shows stability of muon energy and angular distributions of ν_μ interactions in MRD Iron. Both of them are found to be stable within statistical error which imply that neutrino spectrum has been stable.

Absolute number of neutrino interactions is measured by FDs for normalization of SK observation. The 1kt detector gives least systematic error when deriving expected number of events at SK because the interaction target and detection principle are the same. Therefore we use the 1kt result to estimate SK expectation. Of course, both SciFi and MRD can derive the SK expectation, independently. Those results are used for confirmation. Neutrino events in 1kt are selected as follows: a) no detector activity in $1.2 \mu\text{sec}$ before the spill b) analog sum signal of all PMTs shows only single peak greater than 1000 p.e. in a spill time window. c) the reconstructed vertex is inside the 25 t fiducial volume. The criterion a) is to reject delayed activity induced by cosmic rays and b) is to reject spills with multiple interactions. The resulting detection efficiency is 72% (87% for CC interactions). After correction of multiple interactions in a spill, total number of neutrino interactions in 25 t fiducial volume is measured to be 61585. Dividing it by live POT of 1kt, the neutrino interaction rate is $3.2 \times 10^{-15} / 25\text{t}/\text{POT}$.

Čerenkov light from pions was successfully observed by the PIMON as demonstrated in Fig. 9. Relative population in $p_\pi-\theta_\pi$ plane is determined by fitting expected light distribution to the data. The fit results are also shown in the same

figure. It can be seen that the data is fitted well. Using the pion distribution ob-

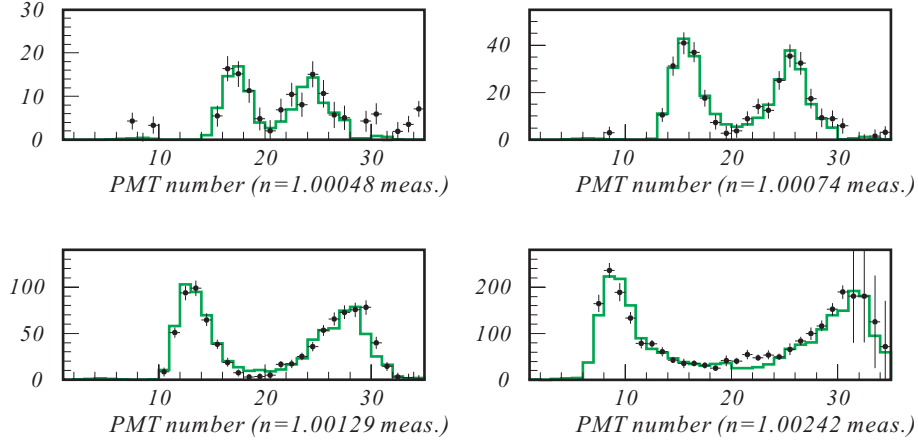


Figure 9: Čerenkov light distribution measured by the PIMON. The points with error bars are data and the solid lines are fit results.

tained by the fitting, neutrino spectra at SK and FD are calculated. Fig. 10 shows ν_μ energy spectrum and the the flux ratio at SK to FD thus obtained with beam Monte-Carlo prediction. We observed very good agreement between PIMON mea-

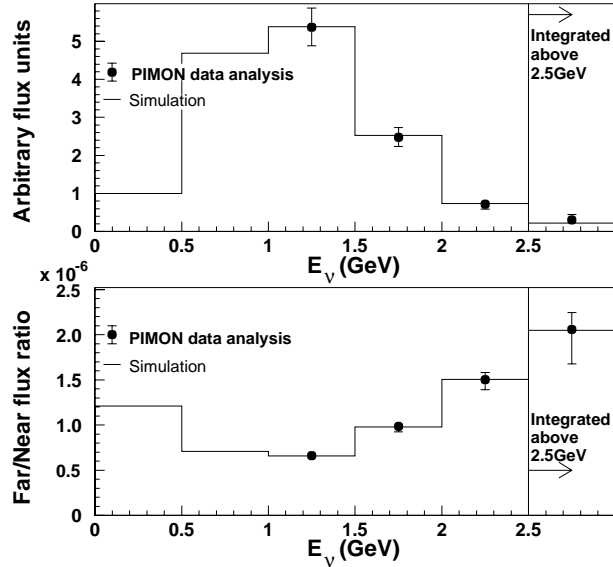


Figure 10: Top figure shows the ν_μ energy spectrum at the near site and the bottom figure show the far to near ν_μ flux ratio. The histograms are from the beam simulation results. The data points are derived from the PIMON measurement.

surements and MC prediction within uncertainty above $E_\nu \geq 1$ GeV. Full description of the PIMON analysis and results are found in ¹¹⁾.

Expected number of events at SK, N_{SK}^{expt} , without neutrino oscillation is

estimated as follows;

$$N_{SK}^{expt} = \frac{N_{1kt}^{obs}}{\varepsilon_{1kt}} \times R_{int} \times \varepsilon_{SK} \quad (9)$$

where N_{1kt}^{obs} is number of selected ν_μ events in 1kt detector, $\varepsilon_{1kt} = 0.72$ is the detection efficiency of 1kt, R_{int} is the ratio of number of interactions in SK to 1kt and $\varepsilon_{SK} = 0.79$ is the detection efficiency of SK. Central value of R_{int} is estimated by MC. The error of the PIMON measurement is taken as its systematic error in the sense that the beam MC is proved within the error of the PIMON measurement. We obtained the expected number of FC events in SK fiducial volume of $37.8_{-3.8}^{+3.5}$. Breakdown of the observed and expected number of events into event categories are listed in Table 1. The statistical uncertainty in the expected number is negligible. Systematic

Table 1: Breakdown of observed and expected numbers of events into event categories.

Category	Obs.	Expected
Total	28	$37.8_{-3.8}^{+3.5}$
1-ring	15	22.9
μ -like	14	20.9
e-like	1	2.0
multi rings	13	14.9

uncertainties are summarized in Table 2. Largest systematic error ($_{-7}^{+6}\%$) is from far/near ratio, and fiducial volume error of 1kt contributes 4%, and both effects of multiple interactions in a single bunch in 1kt and SK fiducial volume error contribute 3%. The observed deficit of neutrino events in SK corresponds to 90% C.L.

Table 2: Summary of systematic errors in expected number of FC events in 22.5 kt.

Far/near ratio	$_{-7}^{+6}\%$
1kt $\Delta V/V$	$\pm 4\%$
Multi events	$\pm 3\%$
Spectrum (ϵ)	$\pm 2\%$
SK(mainly $\Delta V/V$)	$\pm 3\%$
Total	$_{-10}^{+9}\%$

4 Future long baseline experiment — JHF-Kamioka ν project —

4.1 Purpose and Strategy

In the first phase of the project SK will be used as a far detector. The goals of the first phase are precision measurement of oscillation parameters in ν_μ disappearance and discovery of ν_e appearance. Also, we can test $\nu_\mu \rightarrow \nu_\tau$ or $\nu_\mu \rightarrow \nu_s$ oscillation by measuring number of NC interaction in SK. The principal strategy of the experiment is 1) use SK at 295 km distance as a far detector, 2) beam energy is tuned to be at the oscillation maximum, 3) neutrino energy of an event is reconstructed from lepton energy and angle assuming charged current quasi elastic (CCqe) interaction, $\nu_l + n \rightarrow l^- + p$. To tune the neutrino energy at the oscillation maximum for currently allowed Δm_{23}^2 , we need low energy beam of $E_\nu = 0.5 \sim 1.2$ GeV for the distance 295 km. Below ~ 1 GeV, ν_μ interaction is dominated by CCqe interaction. Above ~ 1 GeV, the fraction of the CCqe cross section rapidly decreases and inelastic interaction dominates. The inelastic interactions give background for both ν_μ disappearance and ν_e appearance. Therefore we need narrow band ν_μ beam peaked at ~ 1 GeV with as small high energy tail as possible.

4.2 Neutrino facility and beam

The proton beam is fast-extracted from the 50 GeV PS in single turn and transported to the production target. The design intensity of the PS is 3.3×10^{14} ppp, and repetition rate is 0.292 Hz, resulting in the beam power of 0.77 MW. We define typical 1 year operation as 10^{21} POT. With the design parameters, this POT corresponds to about 130 days of actual operation. At present, we have three options of beam configurations; wide band beam (WBB), narrow band beam (NBB) and off axis beam (OAB). The difference is in the optics for the secondary particles. The WBB uses 2 horns almost same as those in K2K ⁹⁾ to focus secondary pions. The NBB is obtained by just placing a dipole magnet between 2 horns in WBB. Momentum selected pion beam produces monochromatic neutrino beam. The OAB is another option to produce beam with narrow spectrum ¹⁴⁾. The optics is almost same as the WBB. The difference is that axis of the beam optics is declined from the axis toward the far detector by a few degree. With the finite decay angle, the neutrino energy becomes almost independent of pion momentum as a characteristics of Lorenz boost. This makes the spectrum narrow. Fig. 11 shows expected neutrino energy spectra at SK for each beam configurations. Hereafter, NBB with selected pion momentum of $\#$ GeV/c is called LE $\#\pi$ and OAB with the beam axis $\#$

degree declined is called OA $\#^\circ$. Expected numbers of interactions are summarized

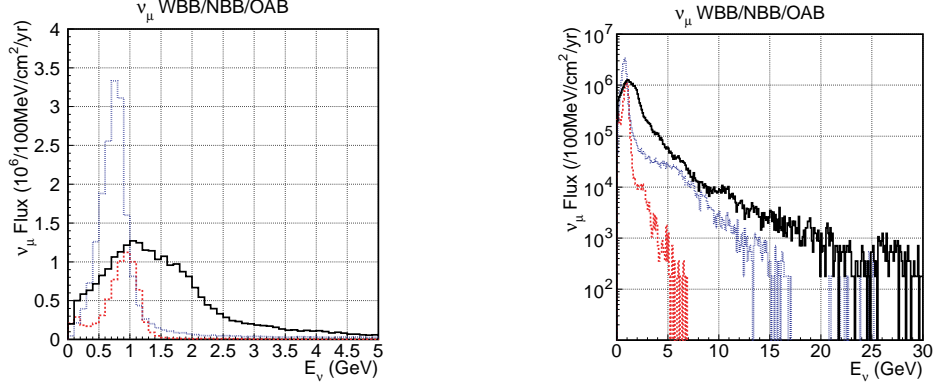


Figure 11: Flux of ν_μ beams. The solid (black), dashed (red) and dotted (blue) lines are WBB, LE 2π and OA 2° , respectively. Differences between the left and right figures are only range of horizontal axis and scale of vertical axis.

in Table 3. LE 2π and OA 2° have sharp peak at ~ 900 MeV and ~ 800 MeV,

Table 3: Summary of ν_μ beam simulation. The second column is peak energy in GeV. The third column is the number of interactions in 1 year in 22.5 kt fiducial volume. The numbers outside (inside) the bracket are total (CC) interactions. The last column is the flux ratio of ν_e to ν_μ in %. The number in the bracket is the ratio at the peak of ν_μ spectrum.

Beam	E_{peak}	$\nu_\mu N_{\text{int}}$	ν_e/ν_μ
WIDE	1.1	7000(5200)	0.74(0.34)
LE1.5 π	0.7	510(360)	1.00(0.39)
LE2 π	0.95	870(620)	0.73(0.15)
LE3 π	1.4	1400(1000)	0.65(0.16)
OA 2°	0.7	3100(2200)	1.00(0.21)
OA 3°	0.55	1100(800)	1.21(0.20)

respectively and WBB has broad peak at ~ 1 GeV. The OAB is roughly factor 3 more intense than NBB. The WBB/OAB have long high energy tail while NBB has rapidly decreasing one. In the ν_e appearance search one of the background sources is ν_e contamination of beam. The sources of ν_e are $\pi \rightarrow \mu \rightarrow e$ decay chain and K decay (K_{e3}). The integrated flux ratios of ν_e to ν_μ are expected to be 0.7%, 0.7% and 1.0% for WBB, LE 2π and OA 2° . At the peak energy of ν_μ spectrum, the ratio decreases as small as 0.2% in the cases of NBB/OAB. This indicates that beam ν_e background in the ν_e appearance search could be greatly suppressed (factor ~ 4) by applying energy window cut in the event selection.

4.3 High precision measurement of Δm_{23} and θ_{23} with ν_μ disappearance

Disappearance of muon neutrinos results in distortion of the ν_μ energy spectrum. Basically, we select FC single ring muon-like events to enrich CCqe interactions. Expected reconstructed neutrino energy (E_ν^{rec}) spectrum at SK with five years exposure of the OA2° without neutrino oscillation is shown in Fig. 12. The spectrum with neutrino oscillation of the parameters $(\Delta m_{23}, \theta_{23}) = (3 \times 10^{-3} \text{eV}^2, \pi/4)$ is also shown in Fig. 12. The spectra of the two cases are quite different. In the

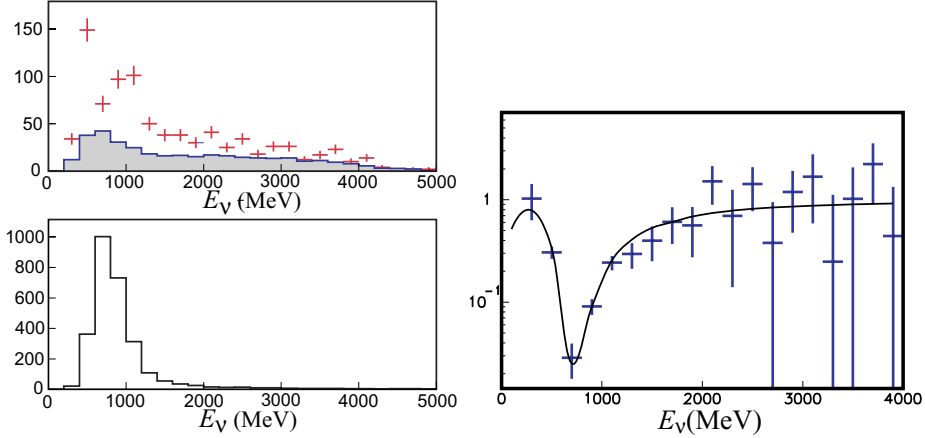


Figure 12: (Left) The E_ν^{rec} spectrum measured in SK for 5 years exposure of OA2°. The top plot is in the case of neutrino oscillation with parameters of $(\Delta m_{23}, \theta_{23}) = (3 \times 10^{-3} \text{eV}^2, \pi/4)$. The contribution of non-qqe interactions is shown by the hatched histogram. The bottom plot is for qqe events in the case of null oscillation. (Right) The ratio of the measured spectrum with neutrino oscillation to the expected one without neutrino oscillation after subtracting the contribution of non-qqe-events. The fit result of the oscillation is overlaid.

oscillation analysis, the ratio of the observed energy spectrum after subtraction of non-qqe background to the expected spectrum without oscillation is fitted by the function of $P(\nu_\mu \rightarrow \nu_\mu)$ to measure the oscillation parameters. The ratio is shown in Fig. 12 with the fit result of $(\Delta m_{23}, \sin^2 2\theta_{23}) = ((2.96 \pm 0.04) \times 10^{-3} \text{eV}^2, 1.0 \pm 0.01)$. The oscillation pattern is clearly seen. Though the error is only statistical, the precision of $\sin^2 2\theta_{23}$ is achieved down to 1% level and Δm_{23} is down to $4 \times 10^{-5} \text{eV}^2$. With OA2°, the maximum sensitivity to the oscillation parameters is achieved at $\Delta m_{23} = (3 \sim 3.5) \times 10^{-3} \text{eV}^2$. Several beam configurations are studied in the range of Δm_{23} between 1×10^{-3} and $1 \times 10^{-2} \text{eV}^2$. The result is summarized in Fig. 13. In consequence, the final sensitivity in JHF experiment can be achieved for $\sin^2 2\theta_{23}$ around 1% level and Δm_{23} below $1 \times 10^{-4} \text{eV}^2$. With a narrow band neutrino beam, the expected systematic uncertainty can be down to the level of the statistical uncer-

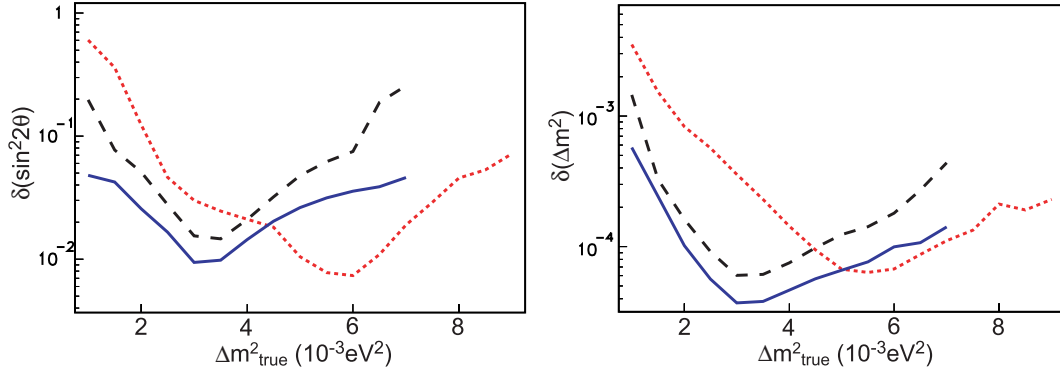


Figure 13: Attainable sensitivity of the neutrino oscillation parameters: $\sin^2 2\theta_{23}$ (left) and Δm_{23}^2 (right), as a function of true Δm_{23}^2 (eV^2). The $\sin^2 2\theta_{23}$ is set to 1.00. The result with OA2° is shown by the blue (solid) line, LE1.5 π by the green (dashed) line and LE3 π by the red (dashed-dotted) line.

tainty with the detailed study of neutrino interactions in a front detector. Previous study for the systematic error is found in the reference ⁴).

4.4 ν_e appearance search

The signal process for the ν_e appearance search is a CCqe interaction $\nu_e n \rightarrow e^- p$. Since proton velocity is usually below the Čerenkov threshold, the signature of the process is a single electromagnetic shower. The background sources are $\nu_\mu \rightarrow \mu$ with e/μ misidentification, beam ν_e contamination, and NC π^0 production where one of the two decay photons is missed. The standard electron selection of the SK atmospheric neutrino analysis is that single, showering (electron like) ring with energy greater than 100MeV, and no decay electrons. After applying the selection the background is dominated by the NC π^0 production. In order to further reduce the background, we developed a new e/π^0 separation algorithm ¹⁵). We forced to find a second ring anyway even though the standard analysis says it is a single ring event. Then we apply cuts on the parameters constructed from the information of those two rings, for example, the energy fraction of the second ring in total energy or invariant mass of the two rings and so on. Eventually, background rejection factor of $\sim 0.2\%$ for the NBB/OAB is achieved.

Fig. 14 (left) shows the reconstructed neutrino energy distributions after the e/π^0 separation cut after 5 years of running with OA2° beam. The oscillation parameters of $\Delta m^2 = 3 \times 10^{-3} \text{ eV}^2$ and $\sin^2 2\theta_{\mu e} = 0.05$ ($\sin^2 2\theta_{13} \simeq 0.1$) are assumed. A clear appearance peak is seen at the oscillation maximum of $E_\nu \sim 0.75 \text{ GeV}$. By integrating the number of events in the energy range between 0.4 and 1.2 GeV, 90% and 3σ limits are derived as a function of the exposure time (the right plot

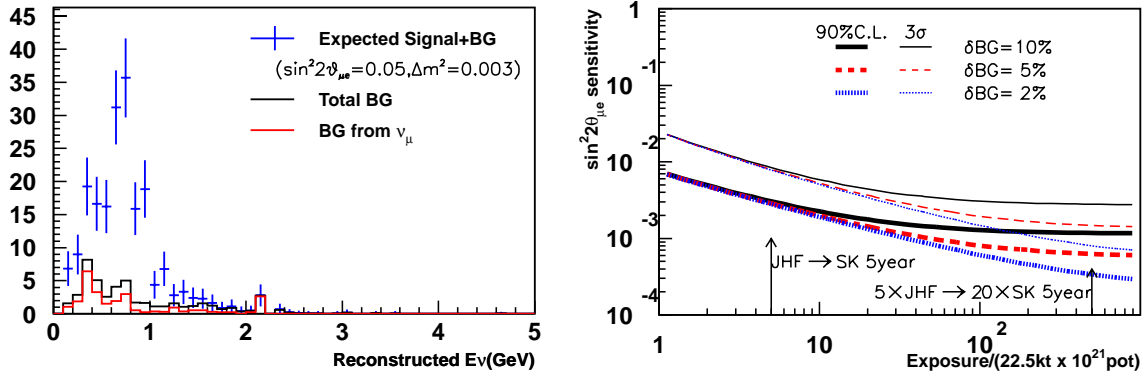


Figure 14: (Left) Expected reconstructed neutrino energy distributions of expected signal+BG, total BG, and BG from ν_μ interactions. (Right) Expected 90% C.L. sensitivity (thick lines) and 3σ discovery (thin lines) contours as the functions of exposure time. The oscillation parameters $\Delta m^2 = 3 \times 10^{-3} \text{ eV}^2$, $\sin^2 2\theta_{\mu e} = 0.05$ are assumed in the left plot. In right plot, Three different contours correspond to 10%, 5%, and 2% uncertainty in the background rate estimation.

of Fig. 14). The reach of the first phase is as good as $\sin^2 2\theta_{\mu e} = 0.003$ at 90% confidence level. The systematic uncertainty in background subtraction is chosen to be 2%, 5% and 10%. At the first phase of JHF exposure, the systematic uncertainty does not make difference. Fig. 15 shows 90% C.L. contours for 5 year exposure of each beam line setups assuming 10% systematic uncertainty in background subtraction. The best sensitivity at around $\Delta m^2 = 3 \times 10^{-3} \text{ eV}^2$ is given by the OA2° beam and the sensitivity is $\sin^2 2\theta_{\mu e} = 0.003$ at 90% C.L. When Δm^2 is significantly larger or smaller than $3 \times 10^{-3} \text{ eV}^2$, sensitivity can be optimized by adjusting the peak energy of NBB/OAB. In the allowed region of $1.6 \times 10^{-3} < \Delta m_{23}^2 < 4 \times 10^{-3} \text{ eV}^2$ by SK atmospheric neutrino data, the 90% confidence level sensitivity is better than $\sin^2 2\theta_{\mu e} = 0.005$ or $\sin^2 2\theta_{13} = 0.01$.

4.5 Neutral Current Measurement

The number of neutral current interaction is proportional to oscillation probability from ν_μ to active neutrinos;

$$N_{NC} \propto P(\nu_\mu \rightarrow \nu_e) + P(\nu_\mu \rightarrow \nu_\mu) + P(\nu_\mu \rightarrow \nu_\tau) - P(\nu_\mu \rightarrow \nu_{sterile}). \quad (10)$$

The probabilities $P(\nu_\mu \rightarrow \nu_e)$ and $P(\nu_\mu \rightarrow \nu_\mu)$ will be known by the measurements of CC interactions as described in the previous sections. If we observe deficit of N_{NC} from expectation, it indicate the existence of sterile neutrino. If not, that means there is no sterile neutrino and we can say that a fraction $1 - P(\nu_\mu \rightarrow \nu_e) - P(\nu_\mu \rightarrow$

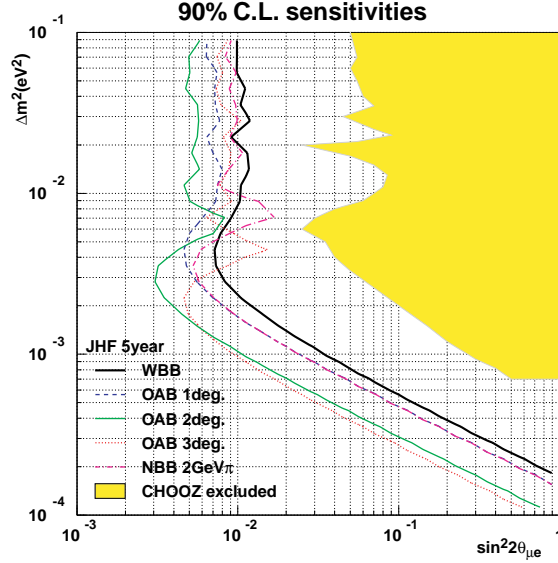


Figure 15: 90% C.L. sensitivity contours for 5 year exposure of WBB, OA1°, OA2°, OA3° and LE2 π configurations. 90% C.L. excluded region of CHOOZ is plotted as a comparison. For CHOOZ contour, maximum mixing of $\sin^2 \theta_{23} = 0.5$ is assumed to convert from $\sin^2 2\theta_{13}$ to $\sin^2 2\theta_{\mu e}$.

ν_μ) of initial ν_μ is oscillated into ν_τ since we know from LEP that the number of light neutrino is 3. In the atmospheric neutrino observation at SK, the possibility of $\nu_\mu \rightarrow \nu_s$ oscillation with full mixing has been excluded with 99% C.L. ¹⁶⁾. We can confirm the results from SK with completely different systematics. It is impossible to do this kind of analysis in K2K experiment due to the limited statistics. The high intensity of the JHF neutrino beam will enable us to use the NC interactions.

Selection criteria for the NC interactions are: 1) fully contained, 2) electron equivalent energy is greater than 100MeV and less than 1500MeV, 3) number of rings is less than 3, 4) all the rings are electron like and 5) no decay electron. After applying these cuts, about 315 events are expected to be observed in one year with WBB configuration in the case of no sterile neutrino. The NC purity of the sample is 88% and ν_μ CC contamination is 9%. If we continue experiment for 5 years with NBB, about 250 events are expected assuming no sterile neutrino. In this case, the purity is 80% and ν_μ CC background is 13%. The expected numbers of events as a function of Δm^2 are shown in Fig. 16. In the figure, maximal mixing is assumed. The systematic error is assumed to be 5%. The expected numbers of events for $\nu_\mu \rightarrow \nu_\tau$ and $\nu_\mu \rightarrow \nu_s$ are clearly separated if the Δm^2 is larger than $\sim 10^{-2.5}$ eV² for both WBB and NBB configurations. From the results of the ν_μ disappearance analysis, we can pin down the Δm^2 within a few percent level quite soon. Then,

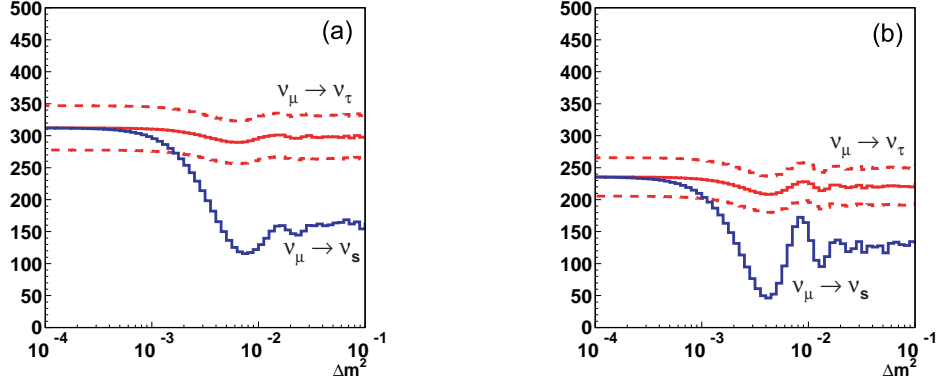


Figure 16: Expected number of events as a function of Δm^2 for (a) 1 year of wide band beam(WBB) configuration and (b) 5 years of narrow band beam(NBB) configuration. The solid lines show the expected numbers of events assuming $\nu_\mu \rightarrow \nu_\tau$ or $\nu_\mu \rightarrow \nu_s$. The dotted lines show the 90% C.L. regions of $\nu_\mu \rightarrow \nu_\tau$ oscillation.

we can compare the obtained experimental results with the two assumptions of oscillation.

4.6 Future extension

In the 2nd phase of JHF neutrino program, the proton intensity is expected to go up to 4 MW. As for the far detector, Hyper-Kamiokande detector is proposed as a next generation large water Čerenkov detector ⁶⁾ at the same place as the SK. The fiducial volume of ~ 1 Mt is being discussed. With these upgrades in both accelerator ($\times 5$) and detector ($\times 40$), the neutrino sensitivity is expected to improve by a factor of 200. The goal of the 2nd phase is

- $\sin^2 2\theta_{13}$ sensitivity below 10^{-3}
- CP phase δ measurement down to 10 - 20°
- Test of the unitarity triangle in the lepton sector
- Search for Proton decay: $p \rightarrow K^+ \bar{\nu}, e^+ \pi^0$

In measuring the CP asymmetry in lepton sector, $\nu_\mu \leftrightarrow \nu_e$ oscillation is known to provide the best chance because the leading term of $\nu_\mu \leftrightarrow \nu_e$ oscillation is highly suppressed due to small Δm_{12}^2 . The CP asymmetry is calculated as

$$A_{CP} = \frac{P(\nu_\mu \rightarrow \nu_e) - P(\bar{\nu}_\mu \rightarrow \bar{\nu}_e)}{P(\nu_\mu \rightarrow \nu_e) + P(\bar{\nu}_\mu \rightarrow \bar{\nu}_e)} = \frac{\Delta m_{12}^2 L}{4E_\nu} \cdot \frac{\sin 2\theta_{12}}{\sin \theta_{13}} \cdot \sin \delta \quad (11)$$

By choosing low energy neutrino beam at the oscillation maximum ($E \sim 0.75$ GeV and $L \sim 295$ km) the CP asymmetry is enhanced while the fake asymmetry due to

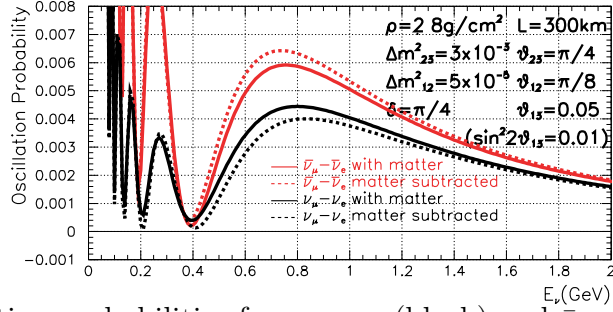


Figure 17: Oscillation probabilities for $\nu_\mu \rightarrow \nu_e$ (black) and $\bar{\nu}_\mu \rightarrow \bar{\nu}_e$ (red). The solid curves includes asymmetry due to matter effect. For the dashed curves, the matter effect is subtracted and the difference between $\nu_\mu \rightarrow \nu_e$ (black) and $\bar{\nu}_\mu \rightarrow \bar{\nu}_e$ (red) are all due to CP effect.

matter effect is small because it is proportional to neutrino energy. In the large mixing angle solution of solar neutrino (LMA), which is favored by the recent SK day-night and spectral results ⁸⁾, the CP asymmetry can be large. Fig. 17 shows oscillation probabilities for $\nu_\mu \rightarrow \nu_e$ (black) and $\bar{\nu}_\mu \rightarrow \bar{\nu}_e$ (red) for the central LMA parameters as an example. The CP asymmetry is as large as 25% and the fake asymmetry due to matter effect is only 5-10%. Fig. 18 shows the numbers of ν_e and

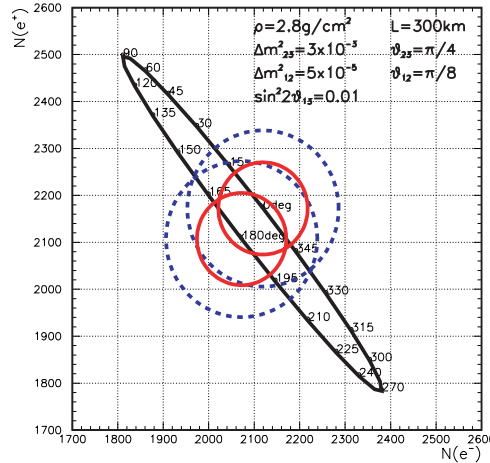


Figure 18: Numbers of ν_e and $\bar{\nu}_e$ appearance events including those from backgrounds is indicated by ellipse as a function δ (degree). Solid circles indicate 90% confidence level (red) contours and dashed circles indicate 3σ contour (blue).

$\bar{\nu}_e$ appearance events including those from backgrounds after 6 years of $\bar{\nu}_\mu$ and 2 years of ν_μ runs in the 2nd phase of the JHF neutrino experiment. CP phase at 0° and 180° correspond to no CP violation. 3σ discovery is possible for $|\delta| \gtrsim 20^\circ$.

5 Summary and Conclusions

The first long baseline neutrino experiment, K2K, has been running since 1999. So far 22.9×10^{18} POT is accumulated. It is demonstrated that neutrino beam is well under control by the observations at KEK site: stability of beam direction, spectrum and intensity. Measurement of the parent pion kinematics just after the production proved the beam simulation. We observed 28 fully contained events in 22.5 kt fiducial volume of Super-Kamiokande. The expected number of event is estimated to be $37.8_{-3.8}^{+3.5}$. The significance of the deficit is 90%.

The next generation long baseline neutrino experiment from ~ 1 MW 50 GeV PS in JHF to SK is planned. The baseline length is 295 km. Low energy beam of ~ 1 GeV with narrow spectrum tuned at the oscillation maximum is used in order to maximize the physics sensitivity. Major goal of the experiment are precise measurement of oscillation parameters and search for ν_e appearance. The expected precision is $\delta(\sin^2 2\theta_{23}) \sim 0.01$, $\delta(\Delta m_{23}^2) \lesssim 1 \times 10^{-4} \text{ eV}^2$. And we can explore ν_e appearance down to $\sin^2 2\theta_{\mu e} \sim 3 \times 10^{-3}$. In the second phase of the experiment with 4 MW upgraded PS and 1 Mt "Hyper-Kamiokande", CPV can be measured if $|\delta| \gtrsim 20^\circ$ in the case of LMA solution. We expect to start experiment in 2007.

References

1. Y. Fukuda et al., Phys. Rev. Lett. **81**, 1562 (1998); K. Kaneyuki, talk presented at 2001 Aspen winter conference on particle physics "PARTICLE PHYSICS AT THE MILLENNIUM", Jan. 2001.
2. See, for example, H.V. Klapdor eds., "Neutrinos", Springer-Verlag, 1988; M. Fukugita and A. Suzuki eds., "Physics and Astrophysics of Neutrinos", Springer-Verlag, 1994; S.M. Bilenky, C. Giunti and W. Grimus, "Phenomenology of Neutrino Oscillations", Prog. Part. Nucl. Phys. **43**,1 (1999).
3. K. Nishikawa et al., KEK-PS E362 proposal, March, 1995; Nucl. Phys. B (Proc. Suppl.) **59**, 289 (1997); S.H. Ahn, S. An, S. Aoki et al., hep-ex/0103001.
4. Y. Itow, et al., "The JHF-Kamioka neutrino project", hep-ex/0106019 (KEK Report 2001-4), June 2001.
5. M. Furusaka, R. Hino, Y. Ikeda, et al., KEK Report 99-4.
6. M. Koshiba, Phys. Rep. **220**, 229 (1992); K. Nakamura, talk presented at Int. Workshop on "Next Generation Nucleon Decay and Neutrino Detector", 1999,

- SUNY at Stony Brook; K. Nakamura, *Neutrino Oscillations and Their Origin*, (Universal Academy Press, Tokyo, 2000), p. 359.
7. M. Kobayashi and T. Maskawa, Prog. Theor. Phys. **49**, 652 (1973); L.-L. Chau and W.-Y. Keung, Phys. Rev. Lett. **53**, 1802 (1984);
 8. S. Fukuda *et al.*, hep-ex/0103032 and hep-ex/0103033 (2001)
 9. Y. Yamanoi *et al.*, KEK Preprint 99-178, Feb. 2000.
 10. H. Noumi *et al.*, Nucl. Instrum. Meth. A **398**, 399 (1997).
 11. T. Maruyama, Ph.D. Thesis, Tohoku University (2000); K2K Beam Monitor Group, in preparation.
 12. A. Suzuki, H. Park, S. Aoki *et al.*, Nucl. Instrum. Meth. A **453**, 165 (2000).
 13. H.G. Berns and R.J. Wilkes, IEEE Trans. Nucl. Sci. 47:340-343 (2000).
 14. D. Beavis, A. Carroll, I. Chiang, *et al.*, Proposal of BNL AGS E-889 (1995).
 15. Y. Obayashi, in Proceedings of the Int. Workshop on “*New Initiatives in Muon Lepton Flavor Violation and Neutrino Oscillation with High Intense Muon and Neutrino Sources*” (2000).
 16. S. Fukuda *et al.*, Phys. Rev. Lett. 85, 3999 (2000)